Journal of Advanced Marine Engineering and Technology, Vol. 50, No. 2, pp. 118~128, 2026
J. Advanced Marine Engineering and Technology (JAMET)
https://doi.org/10.5916/jamet.2026.50.2.118

ISSN 2234-7925 (Print)
ISSN 2765-4796 (Online)
Original Paper

Torsional vibration characteristics and design optimization of a PTO/PTI-based hybrid propulsion system in a wind-assisted ship

Chang-Hyeon Bae[1] · Ji-Min Lee[2] · Mi-So Bae[3] · Yang-Gon Kim[†]

(Received March 22, 2026 ; Revised March 26, 2026 ; Accepted March 30, 2026)

Abstract: In this study, the torsional vibration characteristics of power take-off (PTO)- and power take-in (PTI)-based hybrid propulsion shafting systems were applied to a ship with a wind-assisted propulsion system. Hybrid systems are increasingly being adopted in response to the stringent International Maritime Organization (IMO) greenhouse gas (GHG) regulations. However, integrating multiple power sources complicates shafting structures, necessitating a precise quantitative evaluation of vibration characteristics. In this study, a transfer matrix-based torsional vibration analysis model was established for a propulsion shafting system consisting of a diesel engine, PTO and PTI shaft generators, a two-stage reduction gear, an elastic coupling, and a propeller. The effect of wind-assisted propulsion was considered as a reduction in the equivalent propulsion load, and the torsional responses under engine-only, electric propulsion, and hybrid operating conditions were compared. In addition, a strain-gauge-based telemetry measurement system was installed on a full-scale ship to validate the analytical results. The results showed that the dominant harmonic orders of the propeller shaft torsional stress, namely the third and sixth orders, were consistent between the analysis and measurement, confirming the validity of the model. The measured stresses were approximately 20% those of the analytical results, indicating a conservative model. Under hybrid operation, higher responses were observed in the engine crankshaft, whereas the other components remained within allowable limits. This study verified the reliability of torsional vibration analysis for PTO- and PTI-based hybrid propulsion shafting systems through full-scale validation.

Keywords: Hybrid propulsion system, PTO and PTI shaft generator, Wind-assisted propulsion, Torsional vibration, Design Optimization

Nomenclature

IACS : International Association Classification Society
DWT : Dead Weight Tonnage
GHG : Green House Gas
IMO : International Maritime Organization
MCR : Maximum Continuous Rating
M.O.I. : Moment of Inertia (kgm^2)
PTO : Power Take Off
PTI : Power Take In
J : Mass moment of inertia
L : Left side of the mass moment of inertia
l : Length of connecting rod (mm)
$M_g(\Theta)$: Crank rotational moment due to gas pressure (Nm)
$M_r(\Theta)$: Crank rotational moment due to reciprocating mass (Nm)
m_{rev} : Reciprocating mass (N)
Q_{np} : Exciting torque of propeller blade n order (Nm)
Q_o : Mean propulsion torque of propeller (Nm)
β : Constant (For an even number of blades, $\beta = 0.04 \sim 0.08$, while for an odd number of blades, $\beta = 0.03 \sim 0.07$)
R : Right side of the mass moment of inertia
r : Radius of crank (mm)
T : Internal torque
t : Torsional stiffness coefficient

Greeks symbols

Θ : Displacement
λ : Ratio of connecting rod

† Corresponding Author (ORCID: https://orcid.org/0000-0002-6033-3531): Professor, Division of marine mechatronics, Mokpo National Maritime University, 91, Haeyangdaehak-ro, Mokpo-si, Jeollanam-do, Republic of Korea, E-mail: nvhkim@mmu.ac.kr, Tel: 061-240-7242
1 Senior Vice President, HD Hyundai Samho Co., LTD, E-mail: chbae@hd.com
2 Ph. D. Candidate, Department of marine engineering, Graduate School of Mokpo National Maritime University, E-mail: dlwlals1032@naver.com
3 M. S., Department of marine engineering, Graduate School of Mokpo National Maritime University, E-mail: baemiso2710@naver.com

ω : Rotational angular velocity

1. Introduction

With the strengthening of GHG emission regulations by the IMO and the rapid increase in demand for decarbonization in the shipping industry, various technologies are being developed to improve the energy efficiency of conventional fossil fuel-based propulsion systems. Wind-assisted propulsion technology has gained attention as a promising alternative for simultaneously reducing fuel consumption and mitigating GHG emissions. Recently, wind-assisted propulsion systems have been reported to have the potential to reduce fuel consumption by up to 5–20%, depending on ship operating conditions **[1]**, and the fuel-saving and GHG reduction effects have been empirically verified through actual ship applications. For example, in the case of a wind wing system applied to a bulk carrier, a fuel-saving effect of approximately 10–15% has been reported **[2]**, and in a tanker equipped with rotor sails, fuel savings of approximately 8 %, along with a significant reduction in CO_2 emissions, have been confirmed **[3]**.

When a wind-assisted propulsion system is applied, additional propulsion force variations occur owing to external environmental conditions, such as wind speed and wind direction, which result in propulsion force variations that are different from those of conventional diesel engine-based propulsion systems and may induce different types of dynamic load variations compared to conventional diesel engine-based propulsion systems. However, the existing studies have mainly focused on the energy-saving effects and economic analysis of wind propulsion. Carjova *et al.* analyzed the operational performance and economic feasibility of ships equipped with rotor sails and showed that fuel-saving effects can vary significantly depending on the wind conditions and route characteristics. In addition, it has been suggested that the economic feasibility depends on the installation conditions and operational strategies of the rotor sails **[4]**. Wang *et al.* comprehensively analyzed the application cases and limitations of wind-assisted propulsion technologies and suggested that wind propulsion is an effective technology for reducing the fuel consumption and GHG emissions of ships **[5]**. In particular, various wind propulsion technologies, such as rotor and wing sails, are being applied to actual ships, and fuel savings of approximately 5–20% have been reported depending on the operating conditions and wind environments. In addition, these systems are generally operated in a hybrid form combined with conventional propulsion systems, and their performance is highly dependent on the operating conditions. Recent studies have shown that the effectiveness of wind-assisted propulsion technology is further maximized when applied in combination with conventional propulsion systems rather than as a standalone system. Hybrid propulsion systems based on PTO and PTI integrate the main engine, shaft generator, and electric motor to realize various operating modes and provide high efficiency in terms of energy recovery and reuse. Recently, the concept of a small sailing-type hybrid ship has been proposed, in which wind power is used as the main propulsion source and a diesel engine-based propulsion system is used as an auxiliary power source. In such ships, propulsion is primarily achieved by wind power, whereas under low wind speed conditions or during maneuvering, the conventional engine propeller-based propulsion system operates as a supplementary system. This configuration is characterized by the combined action of a propulsion shafting system consisting of an engine, reduction gear, propulsion shaft, propeller, and wind-based propulsion forces. However, in classification society rules and related standards, wind-assisted propulsion devices are often classified as auxiliary devices rather than as main propulsion systems **[6]**, and torsional vibration analysis of the propulsion shafting system is sometimes not specified as a mandatory requirement. Existing studies have mainly focused on energy-saving effects, economic feasibility, and operational strategies for wind-assisted propulsion systems. Studies on the dynamic effects of such systems on propulsion shafting systems, particularly on the torsional vibration characteristics, remain highly limited. Kim et al. analyzed the torsional vibration characteristics of a propulsion shafting system with a waste heat recovery system and suggested that the excitation torque increases with changes in operating conditions, which may affect the shafting responses **[7]**; however, studies on hybrid propulsion systems combined with wind-assisted propulsion are still insufficient.

Therefore, in this study, the torsional vibration characteristics of a propulsion shafting system for a hybrid propulsion system with wind-assisted propulsion were analyzed, and its dynamic behavior under various operating conditions was investigated. In particular, for a propulsion shafting system, including a PTO- and PTI-based shaft generator system, the effects of torque variations generated under different operating modes on torsional vibration responses were quantitatively evaluated, and fundamental data for a stable propulsion shafting system design were provided.

2. Operational Characteristics of the PTO and PTI-based Hybrid Propulsion System

2.1 Specifications of the Subject Ship

Table 1 and **Figure 1** present the specifications and general

Table 1: Specifications for a subject ship

Item		Detail
Ship type		Wind- assisted cargo ship
Deadweight (DWT)		300
Length (m) x beam (m) x depth (m)		48 x 8.7 x 4.1
Sail type		INDOSAIL system
Sail area (m^2)		500
Max. speed (knot)	Sail system + PTI mode	12
	Hybrid System (Diesel + PTI mode)	7
	Sail system + PTO mode	5

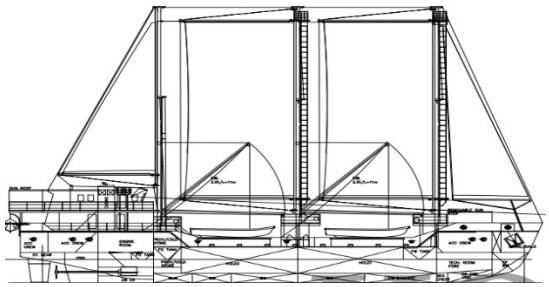

Figure 1: General arrangement of a subject ship

Table 2: Specifications of the propulsion shafting system

Item		Detail
Main Engine	Model	L126TI
	MCR(kw) x rpm	264.8 x 2,000
	Idle power (kW) x rpm	12.67 x 725
	Bore(mm) x stroke(mm)	123 x 155
	Firing order	1-5-3-6-2-4
	Ratio of connecting rod	0.2818
	Reciprocating mass (kg/cyl.)	4.625
	Turning wheel (kgm2)	1.8404
No.1 Reduction Gear	Model	DMT170HL
	Gear ratio	0.168
	Revolution (rpm)	336
No.2 Reduction Gear	Model	PHT420A1S1
	Gear ratio	0.588
	Revolution (rpm)	1,176
Propeller shaft	Diameter (mm)	140
	Material	RSF600M
Propeller	No. of blade	3
	Diameter (mm)	1,850
	MOI in air ($kgcms^2$)	296.75

arrangements of small cargo ships equipped with wind-assisted propulsion technology. Based on this, the subject ship is a wind-propelled cargo vessel of approximately 300 DWT class with a length of 48 m, equipped with a hybrid propulsion system that combines sail-based wind propulsion, electric propulsion, and diesel propulsion. The ship adopts an INDOSAIL-type sail with an effective area of approximately 500 m^2, and can achieve a maximum speed of approximately 12 knots under sufficient wind and solar conditions. In contrast, when wind conditions are limited, propulsion using an electric motor based on a PTI utilizing solar energy, or a hybrid propulsion mode combined with a diesel engine, is used as a supplementary means.

Table 2 lists the main specifications of the propulsion shafting system of the subject ship. Based on this, the propulsion shafting system consists of a propeller, propulsion shaft, two-stage reduction gear, shaft generator performing the functions of the PTO and PTI, electric motor, and diesel main engine. The propeller is a three-blade type with a diameter of approximately 1,850 mm, and the propulsion shaft is designed with a diameter of approximately 140 mm. The reduction gear is configured as a two-stage system with gear ratios of approximately 0.168 and 0.588, and is designed to appropriately transmit the rotational characteristics of the engine and electric motor to the propeller.

The main engine is a four-stroke medium-speed diesel engine with a power output of approximately 264.8 kW, and is characterized by periodic torque acting on the propulsion shafting system according to the firing order. In addition, the electric motor used in the PTO mode provides a relatively constant torque and is used for low-speed operation and auxiliary propulsion.

The subject ship has a multi-source propulsion system in which wind, electrical, and mechanical power act in combination, and is characterized by significant variation in the dynamic characteristics of the propulsion shafting system depending on the operating conditions.

2.2 Operational Concept of the PTO and PTI-based Hybrid Propulsion System

The propulsion system considered in this study is a PTO- and PTI-based hybrid propulsion system that utilizes wind propulsion as the main power source, and electric and diesel propulsion as auxiliary sources. This system has a configuration in which multiple power sources are connected to a single propulsion shaft, and is characterized by changes in the power flow depending on the operating mode. PTO and PTI systems have bidirectional power transmission functions. In PTO mode, electrical power is generated using the rotational power of the propulsion shaft, whereas in PTI mode, additional torque is supplied to the propulsion shaft through an electric motor. These functions are combined with wind propulsion to improve the energy efficiency and provide operational flexibility.

Depending on the operating conditions, the system has the

following main operating modes. First, in the wind-only propulsion mode, the propulsion force generated by the sail enables the ship to sail, and the propeller rotates in seawater by its own hydrodynamic action. The propulsion shafting system connected to the propeller drives the shaft generator via two reduction gears, thereby generating electrical power. The generated power is supplied onboard. In this case, no GHG emissions occur, thus enabling environmentally friendly operations.

Second, in the operating mode, where wind propulsion and electric propulsion are combined, the electric motor is driven by electricity generated from solar energy, together with wind propulsion. At this time, the electric motor generates a relatively constant torque. Third, in the electric propulsion-only mode, propulsion is achieved by the electric motor using electricity generated from solar energy under conditions where wind is insufficient, and relatively stable torque characteristics are obtained. This mode is used for low-speed operations under limited environmental conditions. Fourth, in the hybrid propulsion mode, the main engine and electric motor operate simultaneously, generating a propulsion force. Finally, in the diesel propulsion mode, the propulsion force is generated by the main engine, and the periodic excitation torque owing to the combustion process acts on the propulsion shafting system. However, even in this case, the shaft generator operates to supply onboard electrical power. This mode is primarily used during departures, arrivals, or emergencies.

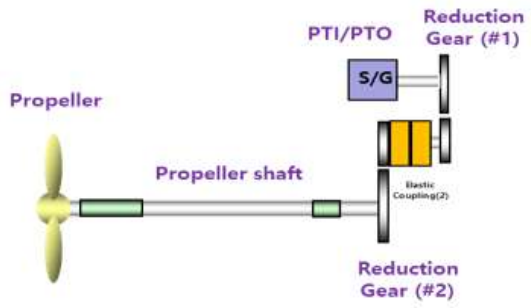

Figure 2: General arrangement of the wind and solar-powered propulsion shafting system (electric propulsion mode)

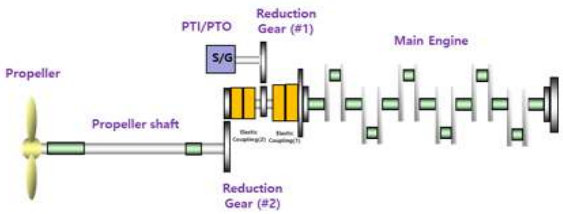

Figure 3: General arrangement of the PTO and PTI based-hybrid propulsion shafting system

The five operating modes described above can be classified into two categories for torsional vibration analysis of propulsion shafting systems, as shown in **Figures 2** and **Figure 3**. They can be divided into an electric propulsion mode based on wind and solar energy, as shown in **Figure 2**, and PTO- and PTI-based hybrid propulsion mode as shown in **Figure 3**.

3. Torsional Vibration Analysis and Experimental Method for the PTO and PTI-Based Hybrid Propulsion System

In this section, a torsional vibration analysis was performed for the propulsion shafting system of a subject ship equipped with a PTO- and PTI-based hybrid propulsion system. The subject ship is a 48 m class wind propelled vessel equipped with major shafting components including the marine diesel engine specified in **Table 2**, and the propulsion shafting system of the ship can be classified into two operating modes as presented in **Figures 2** and **Figure 3**.

3.1 Modeling of the PTO and PTI-Based Hybrid Propulsion System

Because propulsion shafting systems form highly complex vibratory systems, direct analysis of their original state is difficult. Therefore, the system must be replaced by a dynamically equivalent model

Table 3: Specifications of the torsional vibration damper

Item	Detail
Type	Viscous damper
Model	ASK 2699
Outer inertia (kgm^2)	0.0563
Inner inertia (kgm^2)	0.127
Stiffness (MNm/rad)	0.016
Damping coefficient (Nms/rad)	2,900

Table 4: Specifications of the propulsion shafting system

Item		Detail
No.1 elastic coupling	Model	Periflex VN43331
	Inertia (kgm^2)	1.5
	Stiffness (MNm/rad)	0.027
	Relative damping (Ψ)	0.96
No.2 elastic coupling	Model	Rubber block coupling
	Outer inertia (kgm^2)	0.6188
	Inner inertia (kgm^2)	0.1463
	Stiffness (MNm/rad)	0.027
	Relative damping (Ψ)	0.96

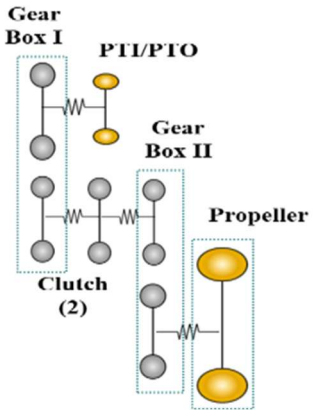

Figure 4: Multi-degree modeling of the wind & solar-powered propulsion shafting system (electric propulsion mode)

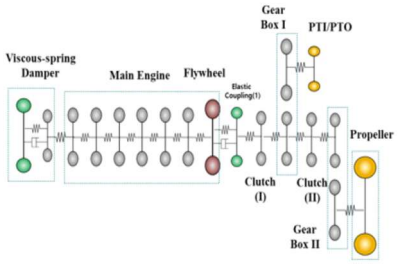

Figure 5: Multi-degree modeling of the PTO and PTI based hybrid propulsion shafting system

consisting of a series of rigid disks representing the mass moments of inertia, and massless uniform cylindrical shafts representing torsional stiffness.

Tables 3 and **4** show the specifications of the viscous-spring damper and the two flexible couplings selected by the shafting designer to control the torsional vibration of the subject ship. Furthermore, **Figure 4** and **Figure 5** illustrate the equivalent mass-elastic models of the propulsion shafting system equipped with the viscous-spring damper and flexible couplings listed in **Tables 3** and **4**.

3.2 Torsional Exciting Torque due to Gas Pressure and Inertial Force

For torsional vibration analysis of the propulsion shafting system, it is necessary to analyze the loads acting on the system in addition to system modeling. On the crankshaft of a marine engine, rotational moments due to the combustion gas pressure in the cylinder and the inertial forces of the reciprocating mass act. Because these vary continuously with a certain periodicity, the rotational moment of the crank throw becomes highly nonuniform. As shown in **Figure 6**, the

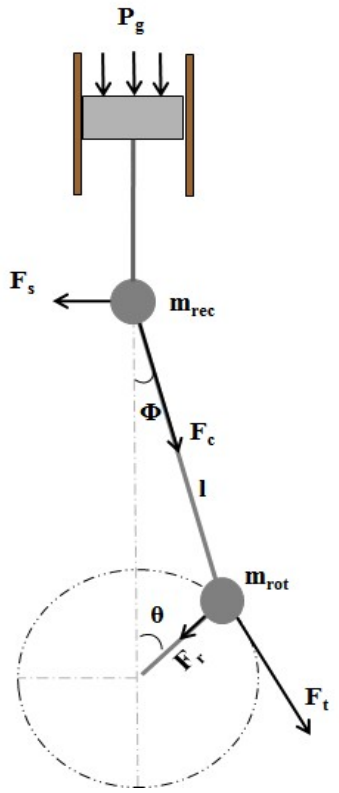

Figure 6: Tangential force of crankshaft

gas pressure acting on the top of the piston rotates the crank through the connecting rod. Here, the tangential force (Ft) becomes the effective force that rotates the crankshaft, and the crank rotational moment due to gas pressure (Mg(θ)) and the rotational moment due to the reciprocating mass (m_{rec}), including the piston and connecting rod, are given by **Equation (1)** and **Equation (2)**, respectively **[8]-[10]**.

$$M_g(\theta) = P_g r(\sin\theta + \frac{\lambda}{2}\sin 2\theta) \quad (1)$$

$$M_g(\theta) = M_{rev}\omega^2 r^2(\frac{\lambda}{4}\sin\theta - \frac{1}{2}\sin 2\theta - \frac{3\lambda}{4}\sin 3\theta - \frac{\lambda^2}{4}\sin 4\theta - \cdots \quad (2)$$

3.3 Propeller Exciting Torque

The propeller excitation torque is generated by variations in the wake field around the propeller, and its magnitude is proportional to the average propeller thrust torque. Similar to the engine-exciting torque, the harmonic analysis shows that the dominant harmonic components correspond to the blade number order and its second and third multiples **[8]**.

$$Q_{np} = \beta Q_0 \sin(n\theta + \psi) \quad (3)$$

3.4 Torsional Forced Vibration Analysis of Propulsion Shafting System using Transfer Matrix Method

Methods such as the modal analysis method, mechanical impedance method, and transfer matrix method are available for forced torsional vibration analysis of a shafting system with multiple degrees of freedom. In this study, the transfer matrix method was adopted because it is more advantageous than the other methods in terms of computational time. The forced vibration equation of the shafting system can be expressed in the matrix form, as shown in **Equation (4) [8]-[10]**, where [J], [C], and [K] are the mass moments of the inertia, damping coefficient, and stiffness coefficient matrices, respectively. where {Q(t)} denotes a vector representing the excitation force.

$$[J]\{\ddot{\theta}\} + [C]\{\dot{\theta}\} + [K]\{\theta\} = \{Q(t)\} \tag{4}$$

The steady-state response due to forced vibration was analyzed using the transfer matrix method as follows: In the torsional vibration system shown in **Figure 7**, the torque between two mass points J_{i-1} and J_i and the torsional angle θ between the mass points are expressed as shown in **Equation (5)**.

$$\begin{aligned} T_i^L &= T_{i-1}^R \,, \\ \theta_i^L &= \theta_{i-1}^R + \frac{T_{i-1}^R}{k_i + j\omega C_i} \end{aligned} \tag{5}$$

Because the solution of the damped forced vibration takes the form of a complex number, it can be separated into real and imaginary parts and arranged as an expanded field matrix, as shown in **Equation (6)**. Here, the superscript (r) denotes the real part, and (i) denotes the imaginary part.

$$\{Z\}_i^R = [P]\{Z\}_i^L \,, \tag{6},$$

$$\begin{bmatrix} \theta^{(r)} \\ T^{(r)} \\ \theta^{(i)} \\ T^{(i)} \\ 1 \end{bmatrix}_i^L = \begin{bmatrix} 1 & \frac{k_{i-1}}{k_{i-1}^2+c_{i-1}^2+\omega^2} & 0 & \frac{c_{i-1}\omega}{k_{i-1}^2+c_{i-1}^2+\omega^2} & 0 \\ 0 & 1 & 0 & 0 & 0 \\ 0 & \frac{-c_{i-1}\omega}{k_{i-1}^2+c_{i-1}^2+\omega^2} & 1 & \frac{k_{i-1}}{k_{i-1}^2+c_{i-1}^2+\omega^2} & 0 \\ 0 & 0 & 0 & 1 & 0 \\ 0 & 0 & 0 & 0 & 1 \end{bmatrix}^L \begin{bmatrix} \theta^{(r)} \\ T^{(r)} \\ \theta^{(i)} \\ T^{(i)} \\ 1 \end{bmatrix}_{i-1}^R$$

Assuming that a sinusoidal torque acts on the ith mass point, the displacement and torque on either side of the mass point can be expressed as shown in **Equation (7)**.

$$\begin{aligned} T_i^R + p_i(\mathrm{t}) &= T_i^L + (-\omega^2 J_i + \mathrm{j}\omega c_i + k_i)\theta_i^L \,, \\ \theta_i^L &= \theta_i^R \end{aligned} \tag{7}$$

By separating the above equation into real and imaginary parts, as in the previous derivation, it can be rearranged into an extended point matrix, as shown in **Equation (8)**.

$$\{Z\}_i^R = [P]\{Z\}_i^L \,, \tag{8}$$

$$\begin{bmatrix} \theta^{(r)} \\ T^{(r)} \\ \theta^{(i)} \\ T^{(i)} \\ 1 \end{bmatrix}_i^L = \begin{bmatrix} 1 & 0 & 0 & 0 & 0 \\ -\omega^2 J + k & 1 & \omega c & 0 & -p(t)^{(r)} \\ 0 & 0 & 1 & 0 & 0 \\ \omega c & 1 & -\omega^2 J + k & 1 & -p(t)^{(r)} \\ 0 & 0 & 0 & 0 & 1 \end{bmatrix}^L \begin{bmatrix} \theta^{(r)} \\ T^{(r)} \\ \theta^{(i)} \\ T^{(i)} \\ 1 \end{bmatrix}_{i-1}^R$$

Therefore, the relationship between the state vector on the right side of the ith mass point and that on the right side of the i−1 th mass point is expressed in **Equation (9)**.

$$\{Z\}_i^R = [P_i][F_{i-1}]\{Z\}_{i-1}^R \tag{9}$$

In this formulation, $[P_i]$ represents the point matrix of the ith mass and $[F_{i-1}]$ denotes the field matrix between the ith and i-1 th masses. Accordingly, the transfer matrix of the entire shafting system was obtained as the product of the field matrices between each mass and the point matrices of each mass, as shown in **Equation (9)**. By substituting the boundary conditions into the state vectors at both ends and performing an analysis, the torsional forced vibration amplitudes and vibration torques at each mass of the propulsion shafting system were obtained.

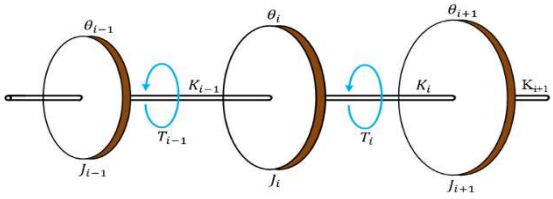

Figure 7: Multi-degree of torsional vibration system

3.5 Measurement Method for Torsional Vibration of the Propulsion Shafting System

Torsional deformation occurs on the shaft surface when a torque is applied to a rotating shaft. In general, this deformation can be detected using strain gauges, from which the torsional exciting torque can be calculated. In this study, full-scale measurements were conducted to validate the torsional vibration analysis results of PTO- and PTI-based hybrid propulsion shafting systems. The measurement target was set as the propeller shaft, and a strain-gauge-based telemetry system was applied to enable real-time measurement of the torsional strain generated during shaft rotation.

Figure 8 shows the measurement system for detecting the torsional strain on the propulsion shaft of the subject ship. The measurement system consisted of strain gauges attached to the propeller shaft surface, a transmitter (TX10K-S) mounted on the shaft, a receiver (RX10K), a tachometer for rotational speed measurement, a reflection tape, signal analysis hardware (OR-35), and analysis software (NV-Gate).

To measure the torsional strain, strain gauges were attached to the outer surface of the propeller shaft, and the measured signals were transmitted wirelessly through a transmitter installed on the rotating shaft. Rotational speed information was obtained using a reflection tape attached to the shaft surface and a tachometer, and this was used as a reference signal to enable the order-tracking analysis. The transmitted strain signals were input to a signal analyzer through a receiver, and the torsional responses in both the time and frequency domains were analyzed using the NV-Gate software. This measurement configuration is considered an appropriate method for the stable measurement of torsional vibration during rotation, considering the characteristics of propulsion shafting systems, where direct wiring to the rotating components is difficult.

During the measurement, data at different rotational speeds were acquired to examine the response characteristics of the torsional stress according to changes in the shaft rotational speed. The measured strain data were converted into torsional stress using the polar moment of inertia of the shaft section and the shear modulus of the material, and at the same time, the overall response and major order components were separated based on the rotational speed signal. To identify the order components that significantly contribute to the additional torsional stress of the propeller shaft, the analysis focused on the 0.5-, 1.0-, 1.5-, 3.0-, and 6.0th order components. The measurement results were organized not only in terms of the overall response but also in terms of each order component so that they could be directly compared with the analysis results.

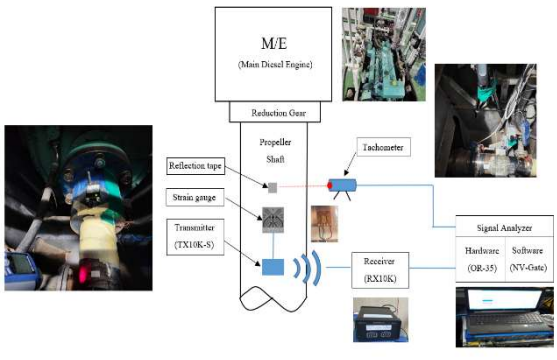

Figure 8: Torsional vibration measurement system

4. Operational Characteristics of the PTO- and PTI-based Hybrid Propulsion System

In this section, the two representative operating modes described in Section 2 are considered to analyze the torsional vibration characteristics of PTO- and PTI-based hybrid propulsion shafting systems. The first is an electric propulsion operating mode in which a shaft generator or an electric motor based on wind and solar energy operates, as shown in **Figure 2**. The second is a PTO- and PTI-based hybrid operating mode, as shown in **Figure 3**. Because the characteristics of the excitation torque acting on the propulsion shafting system differed depending on the operating mode, the corresponding torsional vibration responses were comparatively analyzed.

4.1 Electric Propulsion Operating Mode (PTO and PTI Mode Only)

In this operating mode, in which a shaft generator with PTO and PTI functionalities is used, the system operates either in the PTO mode as a shaft generator or in the PTI mode as an electric motor, with the main engine stopped or partially disengaged. In this case, only the propeller excitation torque is considered in the propulsion shafting system.

Figure 9 presents the results of the forced torsional vibration analysis of the propulsion shafting system shown in **Figure 4** using the transfer matrix method. From these figures, it can be observed that, in the propeller shaft, a torsional stress of 4.24 N/mm² occurs at 471 rpm due to the first mode sixth order component, while in the generator shaft, a torsional exciting torque of 610 Nm occurs at 1,888 rpm due to the third mode sixth order component. In addition, at the input shaft gear of the No.1 reduction gear, a torsional excitation torque of 10 Nm occurs at 1,888 rpm due to the third-mode sixth-order component, whereas at the input shaft gear of the No.2 reduction gear, a torsional excitation torque of 820 Nm occurs at 470 rpm owing to the first-mode third-order component.

These results show that in the electric propulsion operating mode of the subject ship, the hydrodynamic force variation associated with the propeller rotation has a significant influence on the torsional vibration response.

4.2 PTO and PTI-Based Hybrid Operating Mode

This operating mode corresponds to the condition in which a shaft generator with PTO and PTI functionalities and the main diesel engine are simultaneously connected. In this mode, the main diesel engine acts as the primary power source, and a periodic excitation torque is generated owing to the gas pressure produced during the combustion process and the inertial forces associated with the

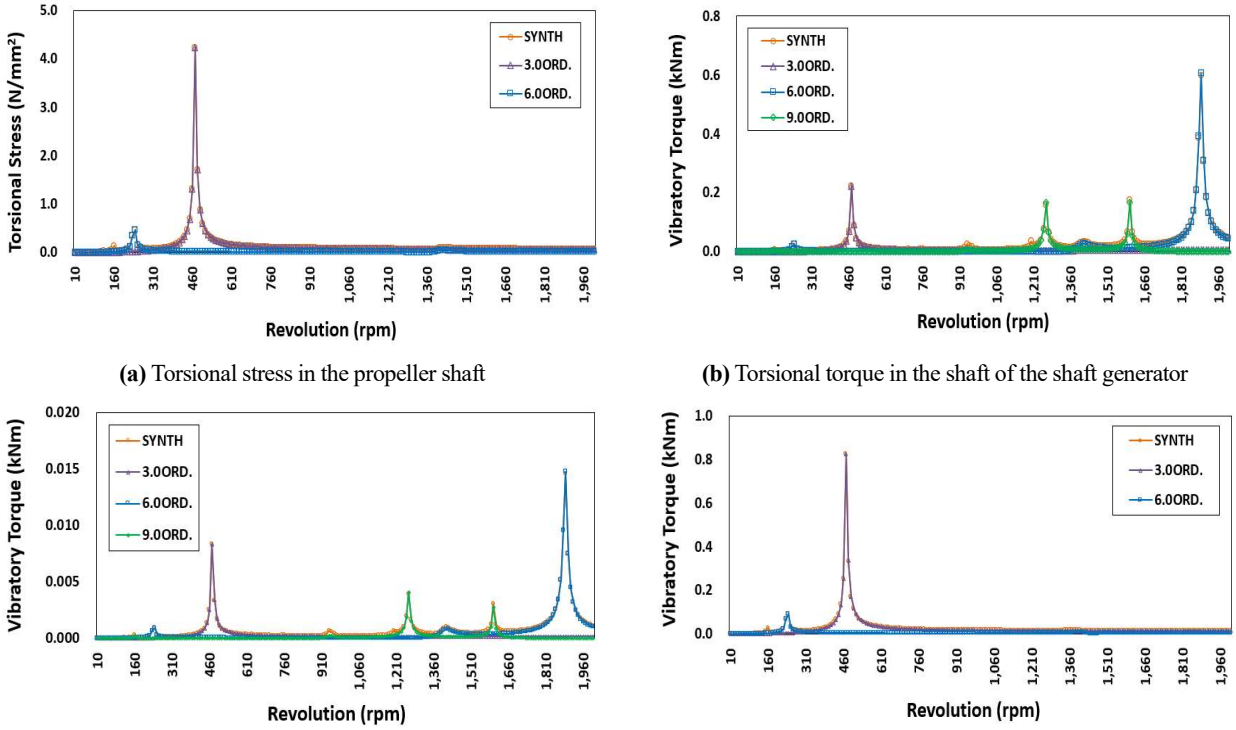

(a) Torsional stress in the propeller shaft

(b) Torsional torque in the shaft of the shaft generator

(c) Torsional torque in the input gear of No.1 reduction gear

(d) Torsional torque in the input gear of No.2 reduction gear

Figure 9: Analysis result of torsional vibration in the wind and solar-powered propulsion shafting system (electric propulsion mode)

reciprocating motion. This torque contains harmonic components of specific orders according to the firing sequence of the engine, and transmits periodic torsional excitation forces to the propulsion shafting system.

Figure 10 presents the results of the forced torsional vibration analysis of the propulsion shafting system shown in **Figure 5** using the transfer matrix method. From these figures, it can be observed that the torsional stress acting on the engine crankshaft system reaches a maximum value of 31.4 N/mm² at No.4 crank throw at 2,000 rpm. Within the operating range, resonance occurs at 1,650 rpm due to the sixth-order component, and the corresponding torsional stress was 11.9 N/mm². In the propeller shaft, high torsional stresses of 38.4 N/mm² and 32.4 N/mm² are observed due to the resonance of the second-mode third- and sixth-order components, respectively. In the generator shaft, a torsional exciting torque of 50 Nm is observed at 1,840 rpm due to the fifth-mode sixth-order component, whereas at 480 rpm, a torsional exciting torque of 60 Nm occurs owing to the second-mode third-order component. At the input shaft gear of the No.1 reduction gear, a torsional exciting torque of 50 Nm occurs at 1,840 rpm due to the fifth mode sixth-order component, and a maximum value of 90 Nm is observed at 480 rpm owing to the second mode third-order component. In contrast, at the input shaft gear of the No.2 reduction gear, a maximum torsional exciting torque of 746 Nm was observed at 480 rpm, owing to the second-mode third-order component.

As described above, in the hybrid operating mode, the third- and sixth-order components act as the dominant excitation sources, which are closely related to the firing cycle of a four-stroke multicylinder diesel engine. In particular, resonance phenomena occur in specific rotational speed ranges, where these order components coincide with the natural frequencies of the propulsion shafting system. Therefore, in the PTO- and PTI-based hybrid operating modes, the torsional vibration responses were dominated by the engine excitation components with a relatively large magnitude and clear periodicity. This behavior is similar to that of conventional direct-driven diesel propulsion systems, indicating that traditional torsional vibration analysis methods can be effectively applied.

4.3 Comparative Analysis of Analytical and Measurement Results in the PTO and PTI-Based Hybrid Operating Mode

The analytical and measurement results of the subject ship were compared and analyzed to verify the validity of the torsional vibration analysis results of the propulsion shafting system. The comparison targets were set as the additional torsional stress and the major order components occurring in the propeller shaft. **Figure 11** presents the torsional response characteristics of the propeller shaft

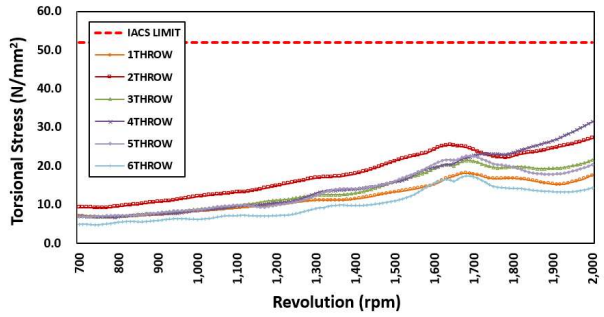

(a) Torsional stress in the all crank throws

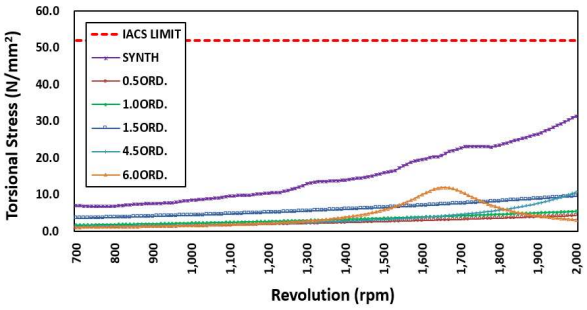

(b) Torsional torque in the No.4 crank throw

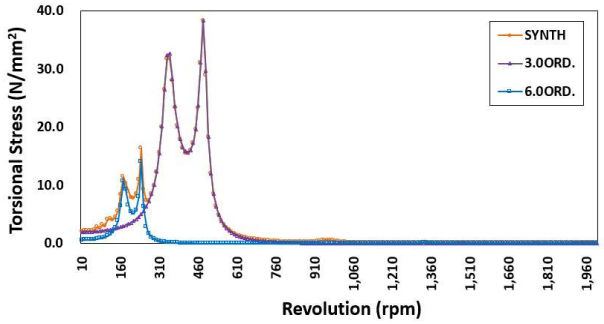

(c) Torsional stress in the propeller shaft

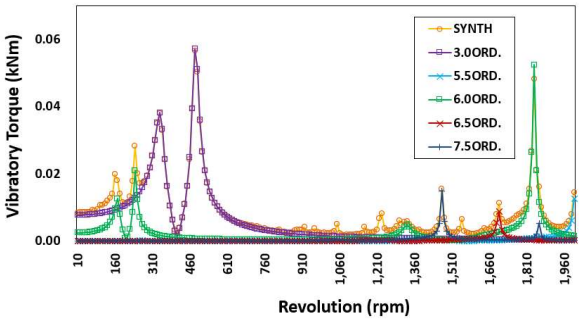

(d) Torsional torque in the shaft of the shaft generator

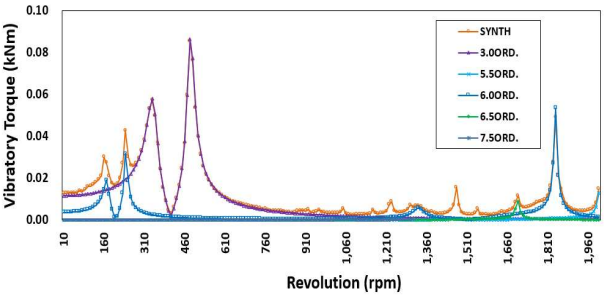

(e) Torsional torque in the input gear of No.1 reduction gear

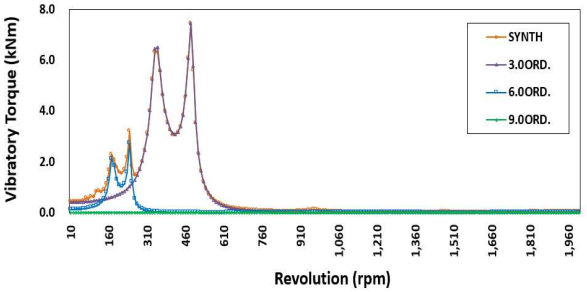

(f) Torsional torque in the input gear of No.2 reduction gear

Figure 10: Analysis result of torsional vibration in the PTO/PTI-based hybrid propulsion shafting system

according to changes in rotational speed. These results indicate that the order components that dominantly affect torsional stress generally exhibit similar tendencies between the analysis and measurement results. In particular, the third- and sixth-order components were identified as the dominant excitation components, indicating that the main excitation source of the torsional vibration in the propulsion shafting system was the engine firing cycle.

The comparison of the torsional vibration response characteristics according to the rotational speed also shows similar trends, and regions where torsional vibration increases at specific rotational speeds are consistently observed in both the analytical and measurement results. This indicates that the locations of the resonance occurrences were appropriately predicted by the analysis. However, differences were observed between the analytical and measured results in terms of the magnitude of the torsional stress. The torsional stress of the propeller shaft obtained from the measurement results was approximately 20% that of the analytical results, indicating that the analysis tended to overestimate the actual values. This difference was attributed to the conservative and excessive evaluation of the engine excitation force in the analysis.

5. Conclusion

In this study, the torsional vibration characteristics of a PTO- and PTI-based hybrid propulsion shafting system with wind-assisted propulsion were analyzed, and the validity of the analytical results was verified through full-scale measurements. In addition, the dynamic

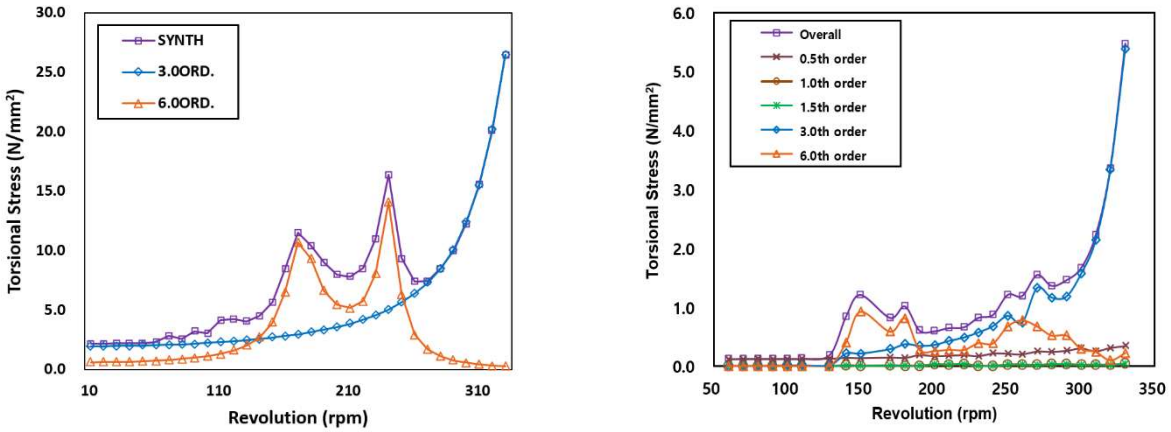

(a) Torsional stress in the propeller shaft

(b) Torsional torque in the shaft of the shaft generator

Figure 11: Comparison of torsional vibration analysis and measurement in the PTO/PTI based-hybrid propulsion shafting system

characteristics according to the operating modes were comparatively analyzed, and the possibility of optimizing the design of the propulsion shafting system was examined.

(1) In the electric propulsion operating mode based on wind and electric power, the exciting torque generated by the hydrodynamic forces of the propeller acts as the dominant excitation source, and the blade-order components govern the torsional vibration response. By contrast, in the PTO- and PTI-based hybrid operating modes, the periodic excitation forces generated by the combustion and inertial forces of the main diesel engine were dominant, and the third- and sixth-order components were identified as the main resonance factors.

(2) In the hybrid operating mode, the engine crankshaft system showed relatively high torsional responses, whereas the responses in the propeller shaft, shaft generator, and reduction gear sections remained below the allowable limits, indicating that structural safety was secured. This implies that sufficient stability in terms of torsional vibration can be achieved, even in hybrid propulsion systems with multiple power sources, if an appropriate design is implemented.

(3) A comparison between the full-scale measurement and analytical results showed that the dominant-order components of the propeller shaft torsional stress (third and sixth orders) appear similar in both results, confirming the reliability of the analytical model. However, the absolute magnitude of the torsional stress in the measurement results was approximately 20% that in the analytical results, indicating that the analytical model had a conservative tendency.

This study is meaningful in that it quantitatively identifies the torsional vibration characteristics of a PTO- and PTI-based hybrid propulsion shafting system with wind-assisted propulsion according to the operating modes and secures the reliability of the analytical model through full-scale measurements. By systematically analyzing the complex excitation characteristics and resulting dynamic responses in a multisource propulsion system, important guidelines for the design and operation of future hybrid propulsion ships are presented.

To better reflect actual operating conditions, future studies must consider torsional vibration analysis under various operating scenarios that account for the dynamic characteristics of the shaft generator driven by hydrodynamically induced propeller rotation during wind propulsion. Furthermore, the proposed analysis and design approach is expected to be applicable to the optimization of the propulsion shafting system design and the establishment of resonance avoidance strategies for eco-friendly hybrid ships.

Acknowledgement

This work was supported by a grant from the National R&D project of “Development of sensors and performance evaluation technology for marine liquid hydrogen storage systems(RS-2024-00437086) funded by Ministry of Trade, Industry and Energy, South Korea. All supports are gratefully acknowledged.

Author Contributions

Conceptualization, Y. G. Kim; Methodology, Y. G. Kim; Software, C.H. Bae; Formal Analysis, C.H. Bae; Investigation, J.M. Lee; Resources, Y. G. Kim; Data Curation M.S. Bae; Writing-Original Draft Preparation, C.H. Bae; Writing-Review & Editing,

Y. G. Kim; Visualization, M.S. Bae; Supervision, Y. G. Kim; Project Administration, Y. G. Kim; Funding Acquisition, Y. G. Kim.

References

[1] European Maritime Safety Agency (EMSA), Potential of Wind Assisted Propulsion for Shipping, Document EMSA/Wind-2022/2023-4837444, Lisbon, Portugal, 2023.

[2] Cargill, "Cargill shares outcome of the world's first wind powered ocean vessel's maiden voyage," Cargill Press Release, Mar. 13, 2024. [Online]. Available: https://www.cargill.com/2024/first-wind-powered-ocean-vessel-maiden-voyage, Accessed March 2026.

[3] Maersk Tankers, "Norsepower rotor sails confirmed savings of 8.2% fuel and associated CO_2 in Maersk Pelican project," Maersk Tankers Newsroom, Oct. 24, 2019. [Online]. Available: https://maersktankers.com/newsroom/norsepower-rotor-sails-confirmed-savings, Accessed March 2026.

[4] K. Carjova, O. P. Hilmola, and U. Tapaninen, "Economic feasibility and operational performance of rotor sails in maritime transport," Sustainability, vol. 17, no. 13, p. 5909, 2025.

[5] K. Wang, Z. Li, X. Liu, Z. Hu, L. Huang, Q. Song, H. Liang, and X. Jiang, "Wind assisted propulsion system for shipping decarbonization: technologies, applications and challenges," Energy, vol. 336, p. 138420, 2025.

[6] Korean Register, Rules for the Classification of Steel Ships, Part 5 Machinery Installations, Busan, Republic of Korea: Korean Register, 2025.

[7] Y. G. Kim, K. H. Cho, and U. K. Kim, "Effects of torsional vibration of a propulsion shafting system using a large scale two stroke marine engine with a waste heat recovery system," Journal of the Korean Society of Marine Engineering, vol. 41, no. 5, pp. 409–417, 2017.

[8] Korean Register, Control of Ship Vibration and Noise, 3rd ed., Busan, Republic of Korea: Textbook Publisher, 2012 (in Korean).

[9] W. K. Wilson, Practical Solution of Torsional Vibration Problems, vol. 1–5, London, United Kingdom: Chapman & Hall, 1942.

[10] J. Nestorides, Handbook of Torsional Vibration, London, United Kingdom: Cambridge University Press, 1958.